# Shared Neural Substrates Controlling Hand Movements in Human Motor Cortex

Jerome N. Sanes,* John P. Donoghue, Venkatesan Thangaraj, Robert R. Edelman, Steven Warach

Voluntary hand movements in humans involve the primary motor cortex (M1). A functional magnetic resonance imaging method that measures relative cerebral blood flow was used to identify a distributed, overlapping pattern of hand movement representation within the posterior precentral gyrus, which contains M1. The observed pattern resembles those reported in nonhuman primates and differs from a somatotopically organized plan typically used to portray human motor cortex organization. Finger and wrist movements activated a wide expanse of the posterior precentral gyrus, and representations for different finger movements overlapped each other and the wrist representation. Multiple sites of activation occurred in the precentral gyrus for all movements. The overlapping representations may mediate motor and cognitive functions requiring coordinated neural processing for finger and wrist actions rather than discrete control implied by somatotopic maps.

Current knowledge about basic features of cerebral cortical organization derives largely from research on animals, but several recently developed techniques allow investigation of the fine details of human cerebral cortical functional organization. Similar to human cerebral cortex, M1 in monkeys has major regions that separately represent the leg, arm, and head in successively more lateral positions along the precentral gyrus (*1*). Converging evidence suggests that, whereas the leg, arm, and head retain separable motor representations, the M1 arm area of nonhuman primates contains multiple, overlapping representations for arm muscles and movements (*2–4*). In contrast, an early view of human M1 organization based on cortical surface electrical stimulation placed proximal arm movement representations medially and those for successively distal movements in discrete, nonoverlapping regions in the lateral part of the arm representation (5). This classical plan also holds that representations of each arm segment have a single, contiguous focus of representation, with, for example, the thumb representation separated from the wrist representation.

Recent imaging studies in humans with positron emission tomography (PET) indicated a segregation of distal and proximal functions for peak activation but showed overlap for entire activation zones of distal and proximal arm representations (6). However, these studies did not adequately evaluate the spatial form of M1 wrist and finger representations in humans. Advances in magnetic resonance imaging (MRI) allow a detailed spatial and temporal description of physiological signals that appear related to neuronal events (*7*, *8*). The organizational pattern of human M1 can potentially be resolved with these high-resolution methods. From the results of a functional MRI method that measures relative parenchymal cerebral blood flow (CBF), we now describe precisely localized but overlapping representations of finger and wrist movements within the human precentral gyrus.

Ten normal, right-handed individuals (9) participated in these experiments. The participants lay supine inside the bore of a 1.5-T magnetic resonance (MR) system (Siemens Medical Systems, Erlangen, Germany) modified for echo planar imaging (*10*). Functional MR images were acquired in the horizontal plane across the frontal lobe while participants used the right hand to perform repetitive flexion-extension movements of either the thumb, index finger, ring finger, or wrist or withheld arm movements (*11*). During these actions, participants were requested to fix gaze and otherwise remain motionless. For this report, we analyzed hemodynamics in the caudal half of the contralateral precentral gyrus (*12*). This region largely contains the primary motor cortex, and we will refer to MR signal intensity as increases in M1 blood flow for a movement versus the no-movement baseline condition.

The cortical region containing the portion of M1 sampled in this experiment exhibited increases of relative CBF when participants performed contralateral hand movements (*13*). Increases in MR signal intensity along the precentral gyrus occurred midway between the lateral and sagittal fissures corresponding to the classically defined arm area of Penfield and Boldrey (5). Along the medial to lateral extent of the left hemisphere, activated sites in the more superior slices generally clustered from the middle to the surface of the precentral gyrus. In contrast, the changes in the MR signal observed in the inferior slices occurred progressively more medially; the fundus of the central sulcus in all 10 participants had label in the most inferior slice exhibiting change in MR signal intensity. For the different movements, there was no difference in the volume of activated tissue (Table 1), and the significantly activated voxels exhibited a 7.9 to 179.1% (74.1 ± 41.1, mean ± SD) increase in MR signal intensity compared with that obtained during no movement. Across participants, the extracted voxels spanned an average of 3.8 ± 0.7 slices or 30.4 ± 5.6 mm along the sampled extent of the precentral gyrus; this region appeared to contain most of the M1 region activated by the tested hand movements (*14*).

Finger and wrist movements activated overlapping volumes of M1 (Fig. 1A). A three-dimensional reconstruction of the activated voxels in M1 revealed a similar pattern of overlap of tissue activated during performance of the different movements (Fig. 1, B and C). The area activated by thumb movements overlapped with 68.0 ± 11.6% of the index finger, 59.7 ± 13.6% of the ring finger, and 52.8 ± 12.3% of the

**Table 1.** Total volume and number of spatially distinct clusters of activated voxels for each movement representation in M1 (mean ± SD). The proportionate size of the largest (primary) and the next largest (secondary) aggregate of contiguous activated voxels relative to each total representation appears in the two right columns. Values represent group means and do not necessarily add to 100. All data are based on changes in MR signal intensity for each movement in comparison with the no-movement baseline condition.

| Movement | Total volume ($mm^3$) | Clusters (*n*) | Primary cluster (% total volume) | Secondary cluster (% total volume) |
|---|---|---|---|---|
| Thumb | 1611.5 ± 547.8 | 3.8 ± 1.6 | 80.6 ± 18.9 | 10.1 ± 8.5 |
| Index | 1549.3 ± 667.0 | 2.4 ± 0.8 | 84.6 ± 20.3 | 9.9 ± 12.8 |
| Ring | 1614.4 ± 754.8 | 3.4 ± 2.2 | 78.6 ± 22.9 | 11.6 ± 13.0 |
| Wrist | 1824.5 ± 849.9 | 3.3 ± 1.3 | 80.7 ± 18.6 | 10.7 ± 8.9 |

J. N. Sanes and J. P. Donoghue, Department of Neuroscience, Division of Biology and Medicine, Brown University, Providence, RI 02912, USA.
V. Thangaraj and R. R. Edelman, Department of Radiology, Beth Israel Hospital, Harvard Medical School, Boston, MA 02115, USA.
S. Warach, Departments of Neurology and Radiology, Beth Israel Hospital, Harvard Medical School, Boston, MA 02115, USA.
* To whom correspondence should be addressed.

wrist representations (*15*). Relative overlap of the remaining representations with each other was comparable in magnitude (range: 49.4 to 62.7%).

M1 representations of individual finger and wrist movements were largely contained within a single contiguous region, such that 81.1 ± 19.6% (range: 33.3 to 100%) of the extracted voxels grouped together. Nevertheless, movement representations for individual subjects typically had additional sites of activation in M1 (Table 1) (*16*), with the second largest cluster comprising 10.6 ± 10.6% (range: 0 to 40.0%) of the extracted voxels. The remaining clusters were small and could contain only a single extracted voxel or as much as 22.2% of a total representation. The change in MR signal intensity during movement for the voxels in the largest cluster was not different from that obtained from voxels in the smaller clusters.

These findings indicate that a large expanse within the human precentral gyrus, the likely location of M1, exhibits activation during individuated finger and wrist movements. These movements activated multiple, overlapping sites and an equivalent cortical volume as previously found in nonhuman primates (*2–4*). The results support the working hypothesis that neurons within the M1 arm area form a distributed and cooperative network that can simultaneously and optimally control collections of arm muscles (*3, 4*), and these results concomitantly provide further evidence against the hypothesis that the M1 arm area contains single, discrete or topographically organized regions for finger or wrist control. The current data also demonstrate the usefulness of functional MRI to derive detailed spatial maps of cerebral cortical regions involved in motor performance. Prior studies with functional MRI indicated that sites located in the vicinity of the precentral gyrus exhibited increased signal intensity during simple, repetitive voluntary hand movements (*7, 17*). Our data confirm these studies and provide details about the functional organization of the major source of cortical output to the spinal cord in humans.

PET investigations of motor cortical organization typically have reported a single, contiguous representation of individual arm segments within M1 (*6, 18*). In contrast, the current data from functional MRI indicate that M1 representations for finger movements as simple as those performed here typically have multiple foci. Representations for the different motor actions appear to share common cerebral cortical tissue, presumably reflecting overlapping functionality within the motor cortical neural network for the arm. The exact significance of this activation pattern remains uncertain, although similarities to emerging theories about cortical organization in macaque M1 (*3, 4, 19*) suggest that finger and wrist movement representations of human M1 share common neural circuitry with more proximal movements. Furthermore, it is likely that the neural elements or ensembles that make up the functional processing units continually recombine while forming new output properties to produce normal and adaptive motor behavior (*20*). Data suggest that an overlapping and distributed neural network represents an efficient mechanism to code motor control variables (*21*). The intermingled representation pattern combined with the profuse horizontal interconnectivity of the various M1 representations (*3*) in primates may help mediate interactions among M1 neurons to coordi-

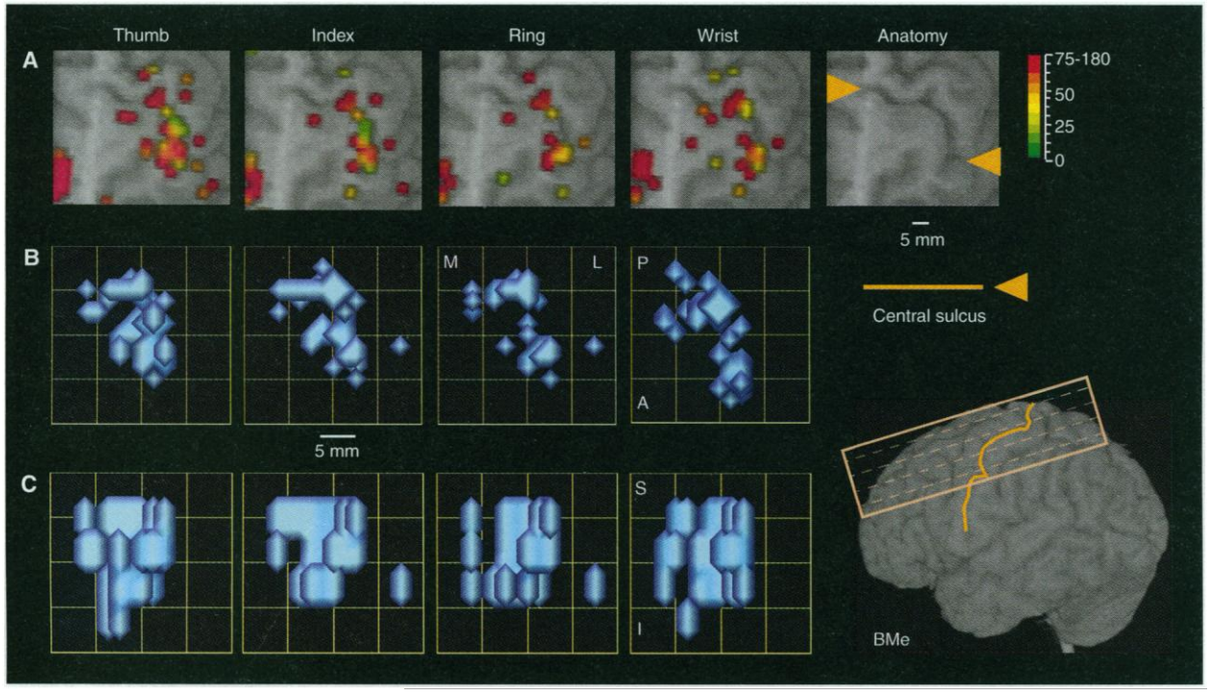


**Fig. 1.** Movement representation overlap in human M1. (**A**) Single-slice depiction of MR signal changes during repetitive finger or wrist movements from one participant. The largest aggregation of extracted voxels was commonly located anterior to the central sulcus (dark curve indicated by yellow arrowheads in "Anatomy" panel) for each movement. MR signal increases in the vicinity of the precentral and postcentral sulci and mesial frontal cortex also occurred during the movements. The view is from the top of the head. In each panel, anterior is down, posterior is up, lateral is to the right, and medial is to the left. The color scale to the right indicates the percentage change in MR signal during movement. (**B** and **C**) Three-dimensional reconstructions of the voxels extracted from M1 (voxels from other cortical areas are not depicted) also showed overlapping movement representations. The voxels extracted from each imaging slice were positioned according to their spatial relationships. The whole-brain image (lower right) indicates the region of cerebral cortex sampled (yellow box), with the dashed lines depicting the center of each imaging slice. Same participant as in (A). In (B) the view angle is from the top of the head as in (A), and the central sulcus "wraps" around the posterior edge of the extracted voxels (from medial to lateral, first above and then to the right of the geometric forms). Note the multiple, separate clusters of voxels with significant activation. P, posterior; A, anterior; M, medial; L, lateral. In (C) the view angle is from the nose such that medial is to the left, lateral to the right, superior is up, and inferior is down. S, superior; I, inferior.

nate reaching and manipulation. Furthermore, the potential for activity-dependent synaptic plasticity among horizontal connections in M1 (*22*) suggests that this overlapping movement representation forms an adaptive and dynamic network to mediate complex motor and cognitive phenomena, such as planning the direction of limb motion and motor skill learning.

*Note added in proof*: Using functional MRI, Rao *et al.* (*23*) describe overlap of hand and elbow representations in a single-slice plane through M1, in agreement with the conclusions presented here.

## REFERENCES AND NOTES


1. C. N. Woolsey *et al.*, *Res. Publ. Assoc. Res. Nerv. Ment. Dis.* **30**, 238 (1952); H. C. Kwan, W. A. MacKay, J. T. Murphy, Y. C. Wong, *J. Neurophysiol.* **41**, 1120 (1978).
2. H. J. Gould III, C. G. Cusick, T. P. Pons, J. H. Kaas, *J. Comp. Neurol.* **247**, 297 (1986); R. J. Nudo *et al.*, *J. Neurosci.* **12**, 2918 (1992).
3. G. W. Huntley and E. G. Jones, *J. Neurophysiol.* **66**, 390 (1991).
4. J. P. Donoghue, S. J. Leibovic, J. N. Sanes, *Exp. Brain Res.* **89**, 1 (1992); M. H. Schieber and L. S. Hibbard, *Science* **261**, 489 (1993).
5. W. Penfield and E. Boldrey, *Brain* **60**, 389 (1937).
6. J. G. Colebatch, M.-P. Deiber, R. E. Passingham, K. J. Friston, R. S. J. Frackowiak, *J. Neurophysiol.* **65**, 1392 (1991); S. T. Grafton, R. P. Woods, J. C. Mazziotta, M. E. Phelps, *ibid.* **66**, 735 (1991); S. T. Grafton, R. P. Woods, J. C. Mazziotta, *Exp. Brain Res.* **95**, 172 (1993).
7. K. K. Kwong *et al.*, *Proc. Natl. Acad. Sci. U.S.A.* **89**, 5675 (1992); S. Kim *et al.*, *J. Neurophysiol.* **69**, 297 (1993); R. T. Constable, G. McCarthy, T. Allison, A. W. Anderson, J. C. Gore, *Magn. Reson. Imaging* **11**, 451 (1993); L. R. Schad, U. Trost, M. V. Knopp, E. Müller, W. J. Lorenz, *ibid.*, p. 461; S.-G. Kim *et al.*, *Science* **261**, 615 (1993).
8. R. R. Edelman *et al.*, *Radiology* **192**, 513 (1994).
9. The participants, nine female and one male (aged 21.2 ± 1.3 years, mean ± SD), were judged strongly right-handed with a modified Edinburgh handedness inventory [R. C. Oldfield, *Neuropsychologia* **9**, 97 (1971)]. Informed consent was obtained according to established Institutional Review Board guidelines.
10. The MR images were acquired by using a circularly polarized head coil for excitation and signal reception. For anatomical localization of functional activity, we acquired T1-weighted parasagittal images with a magnetization-prepared rapid acquisition gradient echo pulse sequence having a 10-ms repetition time, a 4-ms echo time (TE), a 500-ms inversion time (TI), a 256 by 256 matrix with a 280-mm field of view (FOV), and a 200-mm slab thickness divided into 128 partitions for a slice of 1.56 mm with an in-plane resolution of 1.09 mm by 1.09 mm. Functional MR images were obtained in a horizontal plane roughly parallel to the cingulate sulcus by using echo planar imaging with signal targeting and alternating radio frequency [EPISTAR (*8*)]. EPISTAR provides MR signals related to relative CBF and was designed to reveal arterial blood flow changes in response to activation conditions. The EPISTAR functional images had a 128 by 128 matrix, a 16-ms TE, a 950-ms TI, a 320-mm FOV (360 mm for two subjects), and an 8-mm slice thickness to yield an in-plane resolution of 2.5 mm by 2.5 mm and a 50 $mm^3$ volume for a 320-mm FOV (2.81 mm by 2.81 mm and 63.3 $mm^3$ for a 360-mm FOV). Twenty-four images acquired every 1.9 s were averaged for each condition to produce a functional MR image. Functional MR images were obtained successively in 8-mm slices for the activation and control conditions. Head position, which had been stabilized by mild restraint and cushioning, was assessed for movement by comparing anatomic images that had been obtained periodically during the experiment. Analysis of these images revealed that seven subjects exhibited ≤3 mm, two subjects 3 to 5 mm, and one subject 5 to 10 mm of head movement. Functional MR images were reregistered during postprocessing to compensate for these head movements and to minimize mislocalization of active sites.
11. Before imaging, subjects received 5 to 15 min of training to ensure performance of two flexion-extension sequences in 1 s as paced by the sound of the MR system. The training emphasized individuated movement of each finger or the wrist with inaction of other parts of the hand. Finger movements used rotation about the metacarpophalangeal joint. Instructions to begin each task condition were announced through a loudspeaker or earphone system. We acquired functional MR images from the superior cortical convexity and then in successive inferior slices until no hand movement–related activation was observed in simple subtraction images inspected during functional MR image acquisition. If we observed aggregates of active voxels clustered in M1, we obtained three repetitions of each condition, otherwise only one repetition was obtained. Occasionally, because of time constraints, only two repetitions of the movement conditions were done for slices exhibiting active voxels. Functional MR images were obtained in the one or two inferior-most slices while eight subjects performed side-to-side tongue movements.
12. When possible (*11*), we processed an average of the functional MR images acquired from repetitions of each movement condition. For the regional analysis, we measured the mean + 2SD of MR signal intensity outside the brain from an average image obtained during no movement. Voxels in all images having an MR signal less than this value were eliminated. The mean intensity in unsubtracted images was then obtained in M1 and a control region located in the ipsilateral anterior and lateral most portions of each slice. These irregular regions followed and roughly bisected defining sulci and gyri. Within slices, the region remained constant for analysis of each movement condition. For the spatial analysis, we first determined the mean + 2SD noise in the brain space presumably resulting from random fluctuations in blood flow and cognitive actions. This physiological noise was calculated from an image constructed by averaging paired subtraction images of each slice's no-movement condition. A "mask" that used this value was applied to subsequent subtractions of movement and no-movement images to exclude voxels having values less than physiological noise. No spatial filtering was applied to the data. From the resulting images, we counted the number of voxels within each of the defined anatomical regions, calculated areal measurements of activation, and assessed the spatial distribution of voxels exhibiting relative CBF increases.
13. Within M1, movement increased the MR signal intensity 11.2 ± 1.3% (mean ± SD) over that occurring during no movement [probability ($P$) ≤ 0.001, analysis of variance (ANOVA)], with each finger and wrist movement exhibiting more MR signal than that occurring during no movement ($P \leq 0.05$, Scheffé $F$ test). A region in the antero-lateral frontal cortex ipsilateral to the hand movements showed no changes in MR signal associated with the finger and wrist movements. Absence of activation in this region controlled for nonspecific changes in MR signal intensity occurring simply as a result of increased motor activity.
14. In 8 of 10 participants, the most inferior cortical slice either showed no hand movement activation or exhibited activation for both hand and tongue movements. In 9 of 10 participants, the most superior slice also exhibited activation for hand movements, indicating that the hand representation could extend to the most superior portions of the precentral gyrus. However, no activation was observed in contiguous portions of the mesially located paracentral lobule. Tongue movement activated areas in inferior slices, and no overlap occurred for areas activated by tongue and hand movements in seven of eight participants.
15. The overlap of M1 representations was calculated by simple comparison of commonly activated voxels across the different movement conditions.
16. The number of voxel clusters for each movement representation was calculated by grouping voxels together with neighboring borders in the same or adjacent cortical slices. For each body part, we tested the hypothesis that the number of independent clusters in the posterior precentral gyrus equaled one using a Wilcoxon signed rank test. This null hypothesis was rejected for each of the four movements for the grouped data ($P \leq 0.01$).
17. S. M. Rao *et al.*, *Neurology* **43**, 2311 (1993); J. N. Sanes, *Behav. Brain Sci.* **17**, 221 (1994); H. Boecker *et al.*, *Brain* **117**, 1231 (1994).
18. P. E. Roland, B. Larsen, N. A. Lassen, E. Skinhoj, *J. Neurophysiol.* **43**, 118 (1980); P. E. Roland, E. Skinhoj, N. A. Lassen, B. Larsen, *ibid.*, p. 137; M. P. Deiber *et al.*, *Exp. Brain Res.* **84**, 393 (1991).
19. B. J. McKiernan, J. K. Marcario, J. H. Karrer, P. D. Cheney, *Soc. Neurosci. Abstr.* **20**, 983 (1994).
20. K. M. Bennett and R. N. Lemon, *J. Physiol. (London)* **477**, 291 (1994).
21. A. V. Lukashin, G. L. Wilcox, A. P. Georgopoulos, *Proc. Natl. Acad. Sci. U.S.A.* **91**, 8651 (1994).
22. K. M. Jacobs and J. P. Donoghue, *Science* **251**, 944 (1991) ; G. Hess and J. P. Donoghue, *J. Neurophysiol.* **71**, 2543 (1994).
23. S. M. Rao *et al. Neurology* **45**, 919 (1995).


24. Supported by grants from the National Institute on Aging (AG 10634), National Institutes of Neurological Disorders and Stroke (NS 25074 and NS 01634), and the Harcourt General Charitable Foundation.

6 February 1995; accepted 24 April 1995